Semnan University

Journal of Heat and Mass Transfer Research

Journal homepage: http://jhmtr.journals.semnan.ac.ir

Numerical Study of Turbulent Free Convective of Liquid Metal with Constant and Variable Properties in the Presence of Magnetic Field

Mohsen Pirmohammadi*

[a] *Department of Mechanical Engineering, Pardis Branch, Islamic Azad University, Pardis, Iran.*

PAPER INFO

Paper history:
Received: 2018-06-29
Received: 2019-01-16
Accepted: 2019-02-01

Keywords:
Free convection,
Variable properties,
Magnetic field,
Turbulent flow.

ABSTRACT

In this research, turbulent MHD convection of liquid metal with constant and variable properties is investigated numerically. The finite volume method is applied to model the fluid flow and natural convection heat transfer in a square cavity. The fluid flow and heat transfer were simulated and compared for two cases constant and variable properties. It is observed that for the case variable properties in high Hartmann numbers (Ha) the temperature slope near the hot wall is more than the cold wall. For both cases, the temperature gradient near the hot and cold walls is high. By applying magnetic field and increasing the Ha the temperature slope reduces so at Ha=800 the profile is linear. In the case constant properties, the slope of temperature profile near the vertical walls is the same and the temperature profiles pass from one point at the center of the cavity. However,in the case variable properties as it was expected the temperature profile doesn't pass one point and the slope of temperature profile at high Hartmann numbers near the hot and cold walls is partly different. Furthermore, it is indicated that for the case constant properties the Nusselt number is less than the case variable properties.

DOI: 10.22075/jhmtr.2019.15043.1209

1. Introduction

Natural convection in a square cavity has been studied in various energy conversion industries such as electronic industries, heat exchangers, solar collectors and nuclear reactors.

The influence of the fluid properties variation with temperature is essential. The well-known Boussinesq approximation has been extensively applied, but very little research has been done to investigate the influence of variable thermophysical properties in the natural convection heat transfer [1]. Cavity flows with variable properties have been analysed by a number of investigators in the past [1–3]. The study of Leonardi and Reizes [2] was based on vorticity–stream function formulation of the steady-state equations of motion with variable properties. Howbeit, their study was only restricted to gases. They appear to be the first to address the change in the symmetry of Nusselt number distribution curve against cavity length for variable properties. Their result suffered from modified Rayleigh number involving several reference temperatures that was difficult to interpret physically. Zhong et al. [3] obtained a bound for the validity of Boussinesq simplification applied to air with variable properties. They indicated that the effect of increasing thermal conductivity results in the delay of the onset of convection-dominated regime to higher Rayleigh number. Recently, Leal et al. [4] confirmed that the property variation effects are considerable, even well within the assumed region of applicability of Boussinesq approximation, based on the evolution of Nusselt number during the flow development regime. Additionally, they considered air as the working medium. Jin and Chen [5] applied Boussinesq approximation together with variable viscosity which is pertinent to high Prandtl number (highly

* *Corresponding Author: M. Pirmohammadi, Department of Mechanical Engineering, Pardis Branch, Islamic Azad University, Pardis, Iran.*
Email: Pirmohamadi@Pardisiau.ac.ir

nonconducting) fluids. There are some special features connected with the heat transfer in liquid metals/alkali metals (highly conducting) which are not present in other fluids. These have high thermal conductivity and hence low Prandtl numbers. Sarvanan and Kandaswamy [6] examined two-dimensional laminar convection for low Prandtl number liquids. This research was studied in a closed square cavity with different isothermal vertical walls. They displayed that as the thermal conductivity decreases the heat transfer decreases appreciably across the cavity.

Pesso and Piva [7] inquired the free convection of the low Prandtl number fluid with large density differences and Nusselt number was modeled as a function of Rayleigh number.

In some engineering problems such as the manufacturing the semiconductors, superconductors, casting, the magnetic storage media , heat exchanger, Nano fluid flow and the cooling systems of electronic devices, effect of magnetic field on heat transfer is inspected[8-13]. The natural convection of an electrically conducting fluid in an enclosure in the presence of a magnetic field has been thoroughly scrutinized by several researchers in the laminar flow $Ra < 10^6$ [14–19]. Comparatively little attention has been paid to the turbulent flow, $Ra \geq 10^6$, which is of interest for many industrial processes as well.

Numerical study of MHD convection with non-uniform magnetic field in a square differentially heated cavity is investigated by Jalil and Al-Tae'y [20].

They reported that stream functions and isotherms distributions in the cavity are dependent on Rayleigh and Hartmann numbers and also on the magnetic field distribution along the vertical wall.

Kakarantzas et al. [21] inspected numerically laminar and turbulent flow of a liquid metal in a vertical annulus under a horizontal magnetic field. They found that when the magnetic field intensity increases, the regime of flow becomes laminar. Moreover, they observed that the magnetic field causes the flow tends to be axisymmetry.

Liu et al. [22] applied the large-eddy-simulation model for body-fitted grids to inquire the turbulent convection in an ellipsoidal crucible. Numerical comparisons were done for three cases: with a transverse magnetic field, without magnetic field, and with a cusp-shaped magnetic field. They demonstrated that the random thermal fluctuations can be vanished effectively by applying magnetic field.

Numerical simulation of MHD low prandtl number flow between two vertical coaxial cylinders under the effect of internal heating and a horizontal magnetic field was presented by Kakarantzas et al. They exhibited that in for case Ha=0, the flow at $Ra=10^4$ is laminar while for $Ra=10^6$ it is turbulent [23]. Zhang et al. [24] examined two-dimensional turbulent convection in a toroidal duct of a liquid metal blanket of a fusion reactor. They concluded that in stronger mixing and more uniform distribution of wall heat flux, indicating promising potential of this concept of the blanket.

Sajjadi and Kefayati [25] analysed magnetohydrdynamics free convection of water for laminar and turbulent flow in a square cavity numerically by the LBM. They discovered that the heat transfer is increased at $Ra=10^7$ and 10^9 by the rise of Hartmann number from Ha=0 to 25 and also the greatest heat transfer decreasing in the presence of Hartmann number is found at $Ra=10^5$ for Ha=100.

Enayati et al. inspected the natural convection in a differentially laterally heated vertical cylindrical reactor with applying ANSYS FLUENT in a 2-D axisymmetric configuration. The main goal of this paper was to define and study the boundaries of the transitional flow regime leading to turbulent flow for this thermal configuration. Seven cases for a range of Rayleigh numbers from 750 to 8.8×10^8 were studied by using the FLUENT k–ω SST turbulent model [26].

Turbulent MHD convection with variable properties has not been studied yet. In this work, the problem of turbulent MHD convection in a differential heated cavity is numerically solved for different Hartmann numbers, $Ra=10^7$, applying liquid metal as working fluid. Fluid flow and heat transfer for the constant and variable properties are examined and their results are compared to each other.

2. Basic Equation

Fig. 1 depicted the geometry of the present work. It is a two-dimensional cavity with height H.

The vertical walls are in different temperatures and horizontal walls are adiabatic.

Horizontal magnetic field is applied across the cavity.

Dimensionless variables are defined as:

$$Y=\frac{y}{H}, U=\frac{uH}{\propto}, V=\frac{VH}{\propto}, P=\frac{PH^2}{\rho\alpha^2}, X=\frac{x}{H} \quad \varepsilon^*=\frac{\varepsilon H^4}{\propto^3} \quad \sigma^*=\frac{\sigma}{\sigma_r}$$
$$\mu_{eff}^*=\frac{\mu_{eff}}{\mu_r} \quad \theta=\frac{T-T_c}{T_{h-}T_c} \quad \mu_t^*=\frac{\mu_t}{\mu_r} \quad \Gamma_{eff,k}^*=\frac{\Gamma_{eff,k}}{\mu_r} \quad \kappa^*=\frac{\kappa H^2}{\alpha_r^2} \quad (1)$$
$$\Gamma_{eff,\varepsilon}^*=\frac{\Gamma_{eff,\varepsilon}}{\mu_r} \quad \Gamma_{eff,t}^*=\frac{\Gamma_{eff,t}}{k_r}$$

Where u and v are the velocity components, p is the pressure, T is the temperature, α is the thermal diffusivity, ρ is the density, $\mu_{eff}=\mu+\mu_t$, $\Gamma_{eff,t}=k_r+\frac{\mu_t c p_r}{\sigma_t}$, $\Gamma_{eff,k}=\mu_r+\frac{\mu_t}{\sigma_k}$ and $\Gamma_{eff,\varepsilon}=\mu_r+\frac{\mu_t}{\sigma_\varepsilon}$. μ_t is turbulent viscosity that related to $k$and ε[27].

Also μ is the dynamic viscosity, k is the thermal conductivity, c_p is specific heat capacity and σ is the electrical conductivity. The thermos-physical properties vary with temperature as follows [28]:

$$k=91.752-48.688\times10^{-3}T-0.303\times10^{-6}T^2$$
$$C_p=1437.08-580.6\times10^{-3}T+29.02\times10^{-6}T^2$$
$$\sigma=(13.11-33.44\times10^{-3}T+29.02\times10^{-6}T^2)\times10^6 \quad (2)$$
$$C_p=1437.08-580.6\times10^{-3}T+4624\times10^{-6}T^2$$

The governing equations are illustrated in dimensionless form as follows [29]:

$$\frac{\partial U}{\partial X}+\frac{\partial V}{\partial V}=0 \quad (3)$$

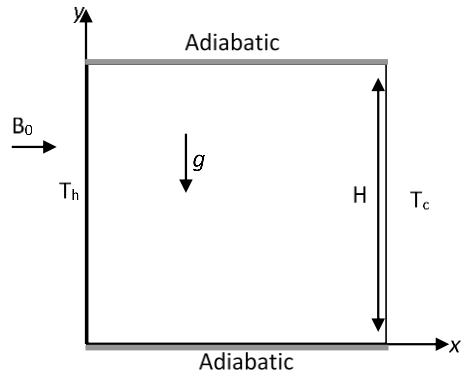

Figure 1. Geometry and coordinates of cavity configuration with magnetic effect

$$U\frac{\partial U}{\partial X}+V\frac{\partial U}{\partial Y}=-\frac{\partial P}{\partial X}+2Pr\frac{\partial}{\partial X}\left(\mu_{eff}^{*}\frac{\partial U}{\partial X}\right)+\Pr\frac{\partial}{\partial Y}(\mu_{eff}^{*}\frac{\partial U}{\partial Y}+\mu_{eff}^{*}\frac{\partial V}{\partial X}) \quad (4)$$

$$U\frac{\partial V}{\partial X}+V\frac{\partial V}{\partial Y}=-\frac{\partial P}{\partial Y}+Pr\frac{\partial}{\partial X}\left(\mu_{eff}^{*}\frac{\partial V}{\partial X}+\mu_{eff}^{*}\frac{\partial U}{\partial Y}\right)+2\Pr\frac{\partial}{\partial Y}\left(\mu_{eff}^{*}\frac{\partial V}{\partial Y}\right)+RaPr\theta-Ha^{2}PrV \quad (5)$$

$$\frac{\partial(c_p^{*}U\theta)}{\partial X}+V\frac{\partial(c_p^{*}V\theta)}{\partial Y}=\frac{\partial}{\partial X}(\Gamma_{eff,t}^{*}\frac{\partial\theta}{\partial X})+\frac{\partial}{\partial Y}\left(\Gamma_{eff,t}^{*}\frac{\partial\theta}{\partial X}\right) \quad (6)$$

$$\frac{\partial(U\kappa^{*})}{\partial X}+\frac{\partial(V^{*}\kappa^{*})}{\partial Y}=Pr\frac{\partial}{\partial X}\left(\Gamma_{eff,k}^{*}\frac{\partial\kappa^{*}}{\partial X}\right)+\Pr\frac{\partial}{\partial Y}\left(\Gamma_{eff,k}^{*}\frac{\partial\kappa^{*}}{\partial Y}\right)+\mathrm{P}_{\kappa}^{*}+\mathrm{G}_{\kappa}^{*}-\varepsilon^{*} \quad (7)$$

$$P_{\kappa}^{*}=2Pr\mu_{t}^{*}\left[(\frac{\partial U}{\partial X})^{2}+(\frac{\partial V}{\partial Y})^{2}+(\frac{\partial U}{\partial X}+\frac{\partial V}{\partial X})^{2}\right]$$

$$G_{\kappa}^{*}=-\frac{\mu_{t}^{*}}{\sigma_{t}}RaPr^{2}\frac{\partial\theta}{\partial Y}\text{-}\varepsilon^{*}$$

$$\frac{\partial(U\kappa^{*})}{\partial X}+\frac{\partial(V^{*}\varepsilon^{*})}{\partial Y}=\frac{\partial}{\partial X}\left(\Gamma_{eff,\varepsilon}^{*}\frac{\partial\varepsilon^{*}}{\partial X}\right)+\quad\frac{\partial}{\partial Y}\left(\Gamma_{eff,\varepsilon}^{*}\frac{\partial\kappa^{*}}{\partial Y}\right)+\mathrm{P}_{\varepsilon}^{*}+\mathrm{G}_{\varepsilon}^{*}-D_{\varepsilon}^{*} \quad (8)$$

$$P_{\varepsilon}^{*}=C_{1}\left[2\mu_{t}^{*}\left[(\frac{\partial U}{\partial Y})^{2}+(\frac{\partial V}{\partial Y})^{2}+(\frac{\partial U}{\partial Y}+\frac{\partial V}{\partial X})^{2}\right]\right]Pr\frac{\varepsilon^{*}}{\kappa^{*}}$$

$$G_{\varepsilon}^{*}=C_{1}C_{3}RaPr^{2}(\frac{\mu_{eff}^{*}}{\sigma_{t}}\frac{\partial\theta}{\partial Y})\frac{\varepsilon^{*}}{\kappa^{*}},\ D_{\varepsilon}^{*}=C_{2}\frac{\varepsilon^{*2}}{\kappa^{*}}$$

Pr, Ra, and Ha are the Prandtl, Rayleigh and Hartmann numbers, respectively are defined as follows:

$$\Pr=\frac{\nu}{\alpha},\ \mathrm{Ra}=\frac{g\beta(T_h-T_c)H^3}{\alpha\upsilon},\ \mathrm{Ha}=B_0H\sqrt{\frac{\sigma}{\rho\upsilon}} \quad (9)$$

Also the used constants in above equations are presented in Table 1 as follows:

The local and average Nusselt numbers are defined as follows:

$$Nu_y=-\left.\frac{\partial\theta}{\partial X}\right|_{X=0}\quad\overline{Nu}=\int_0^1 Nu_y dY \quad (10)$$

Boundary conditions are:

$$\mathrm{U}\,\&\,\mathrm{V}=0\ \text{at all walls}\,(\mathrm{X}=0,\mathrm{X}=1,\mathrm{Y}=0,\mathrm{Y}=1) \quad (11)$$

$$\theta(0,Y)=1,\theta(1,Y)=0,\ \left.\frac{\partial\theta}{\partial Y}\right|_{Y=0}=0,\ \left.\frac{\partial\theta}{\partial Y}\right|_{Y=1}=0 \quad (12)$$

Also wall functions are applied for turbulent parameters as follows [29]:

Table 1. Constants used in $k-\varepsilon$ model.

C_1	C_2	C_3	C_μ	σ_k	σ_t	σ_ε
1.44	1.92	$\tanh(\lvert\frac{v}{u}\rvert)$	0.09	1.0	1.0	1.3

Table 2. Results of $\overline{Nu}$ for different mesh sizes (Ra=107 and Ha=100)

Mesh Size	$\overline{Nu}$
51×51	102
91×91	3.199
101×101	3.187
121×121	3.183
131×131	3.182
141×141	3.182

$$y^{+}=\rho\frac{C_{\mu}^{1/4}\acute{\kappa}^{1/2}}{\sigma_t\left[\left(\frac{1}{\acute{\kappa}}Ln(Ey^{+})\right)+CT\right]}y_p,\ \acute{\kappa}=0.41$$

$$T^{+}=-\rho\frac{C_{\mu}^{1/4}\acute{\kappa}^{1/2}}{\sigma_t\left[\left(\frac{1}{\acute{\kappa}}Ln(Ey^{+})\right)+CT\right]} \quad (13)$$

$$CT=9\cdot24\left[1+0\cdot28Epx\left(-0\cdot007\frac{Pr}{\sigma_t}\right)\right]\left[(\frac{Pr}{\sigma_t})^{1/4}-1\right] \quad (14)$$

3. Numerical Method

The present computation uses the finite volume method and the SIMPLER algorithm to discretize the governing equations of flow and resolving the pressure-velocity coupling system. The hybrid-method is applied to discretize the convection terms [30]. The residual values have been examined for parameters such as velocity, temperature and pressure. Convergence is contemplated to be achieved when residuals become less than 10-3. A staggered grid system is applied. The solution of the fully coupled discretized equations is obtained iteratively applying the TDMA method [30]. For checking the grid independency, the simulations were done for cell numbers from 51×51 to 141×141 for Ra=10^7 and Ha=100. It was detected that using the 121×121 mesh leads to the grid independent result. In Tab. 1 the results of $\overline{Nu}$ at the hot wall are presented. As it is observed, changing the grid from 101×101 to 121×121 will make approximately 0.004 difference in the mentioned results. According to the grid dependency analysis, all results portrayed from now on, are generated by 121×121 grid (table. 2).

4. Validations

For assessing the accuracy of our numerical procedure, we have tested our algorithm vs. a simulation for natural convection flow (without imposed magnetic field) in a square cavity for Ra = 10^{10}, Ha=0 and Pr=0.01 which were reported by jalil [20].

Fig. 2 depicted the streamlines and isotherms for the present work and the results published by Jalil. In this comparison the properties of fluid were assumed to be constant. It is perceived that results exhibit good agreement with results presented in [20].

5. Results and discussion

Turbulent natural convection heat transfer of molten sodium inside a cavity in the presence of magnetic field is

investigated. The Rayleigh number 107and different Hartmann numbers for the cases constant and variable properties are considered.

Figures 3 and 4 illustrated the isotherms in different Hartmann numbers and Ra=107 for the cases constant and variable properties, respectively. It is observed that for both cases when Ha=0 boundary layer is formed near the vertical walls and the isotherms outside the boundary layer are skewed. As Ha increases the temperature gradient near the hot and cold wall decreases and the slope of the isotherms at the centre of the cavity change. At Ha=200 the isotherms become horizontal and with increasing the Ha the isotherms become vertical, so that at Ha=800 the thermal boundary layer is vanished and mechanism of heat transfer changes from convection to conduction.

Regarding the fact that in the case variable properties, the thermal conductivity near the hot wall is less than the cold wall and also in high Hartmann numbers the conduction heat transfer is dominant the temperature gradient near the hot wall is more than the cold wall. As difference between the thermal conductivity of the fluid near the vertical walls enhances the temperature gradient near the hot wall at high Hartmann number increases.

Figures 5 and 6 present the streamlines in different Hartmann numbers for constant and variable properties, respectively. For both cases, when Ha is zero or low in addition to primary vortex, three vortices are formed.

As Ha boosts the secondary vortices disappear and the Lorentz force causes the axes of main vortex rotates and becomes nearly parallel with vertical wall. As Ha increases absolute maximum of stream function decreases. Moreover, it is observed that for the case variable properties the stream lines are not symmetric and concentration of them near the hot wall is more than the cold wall.

This is because near the hot wall the kinematic viscosity and the electrical conductivity is less than the cold wall so viscose and Lorentz forces in this region are less and more flow pass through this region and streamlines become asymmetric. Figure 7 portrayes the velocity profile in different Hartmann for constant and variable properties.

In the case constant properties, the velocity is symmetric and as Ha increases the maximum velocity decreases, however in the case variable properties when Ha=0 the velocity profile is symmetric and as Ha boosts it becomes asymmetric. When Ha=0, the order of buoyancy force is less than the viscous force and difference viscosity doesn't effect on velocity profile, still as Ha increases for the reason that the Lorentz force become higher so that the buoyancy force is more important and the difference of viscosity effects on the velocity profile, so that near the hot wall the maximum velocity is more than the cold wall.

Additionally, near the hot wall electrical conductivity is less compared to the left wall and so it causes the Lorentz force reduces in this region. Figure 8 depicts the temperature profile in different Hartmann numbers for constant and variable properties.

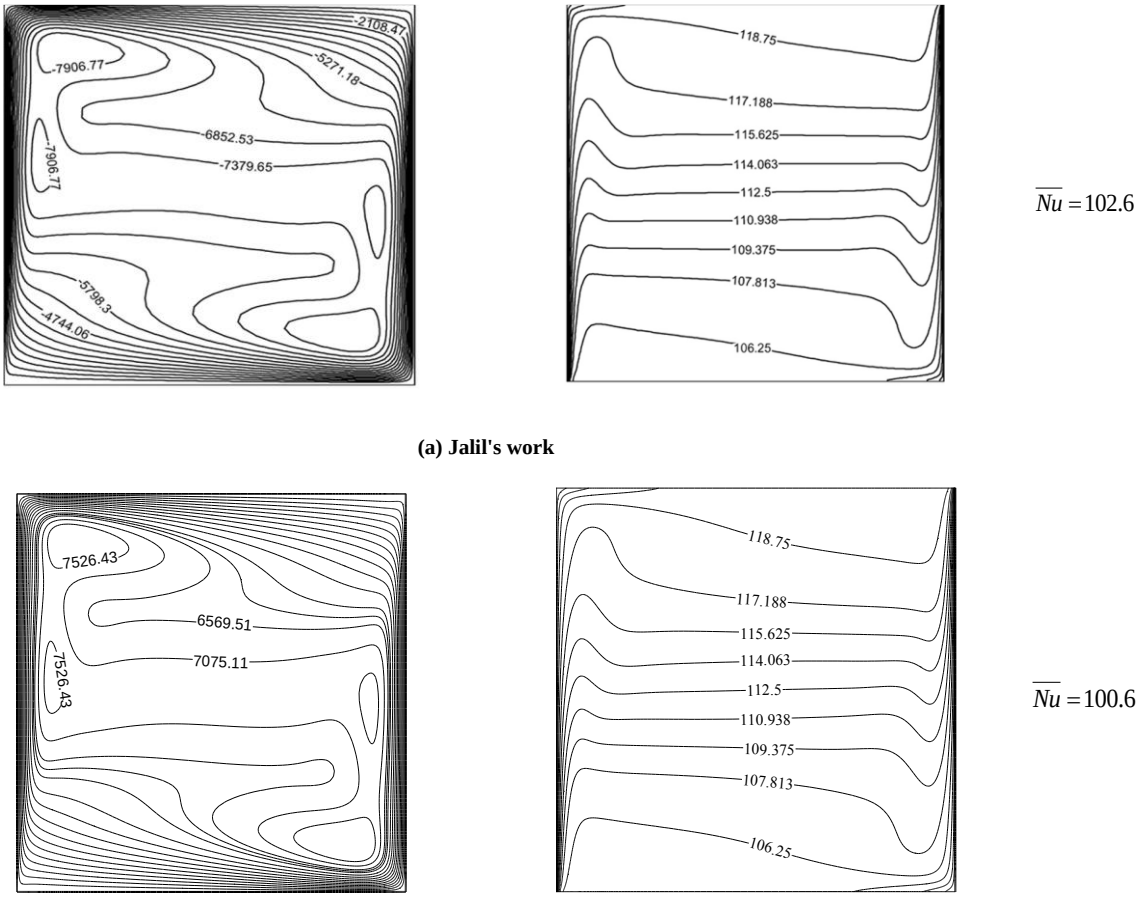

Figure 2. (a) Isotherms and (b) Streamlines of natural convection in a square enclosure for Ra = 10^{10} and Ha=0 (the fluid propertyes are constant)

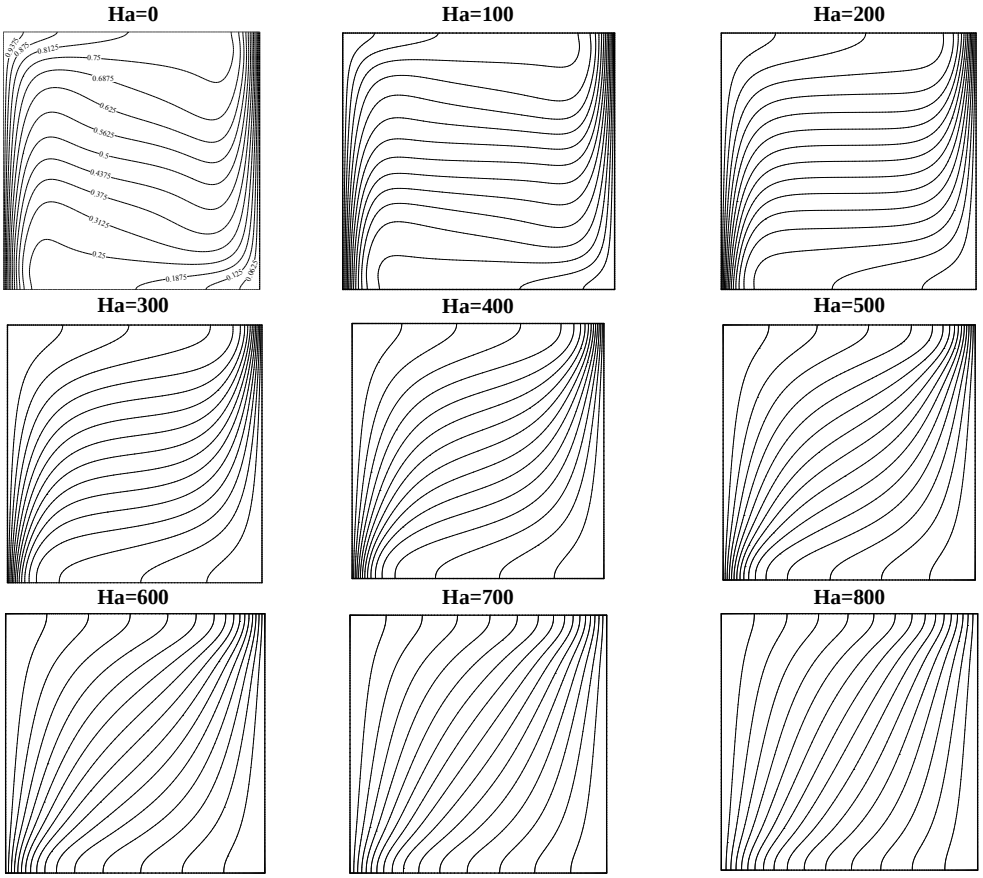

Figure 3. Isotherms for Ra = 10^7 and different Hartmann numbers; the fluid properties are constant

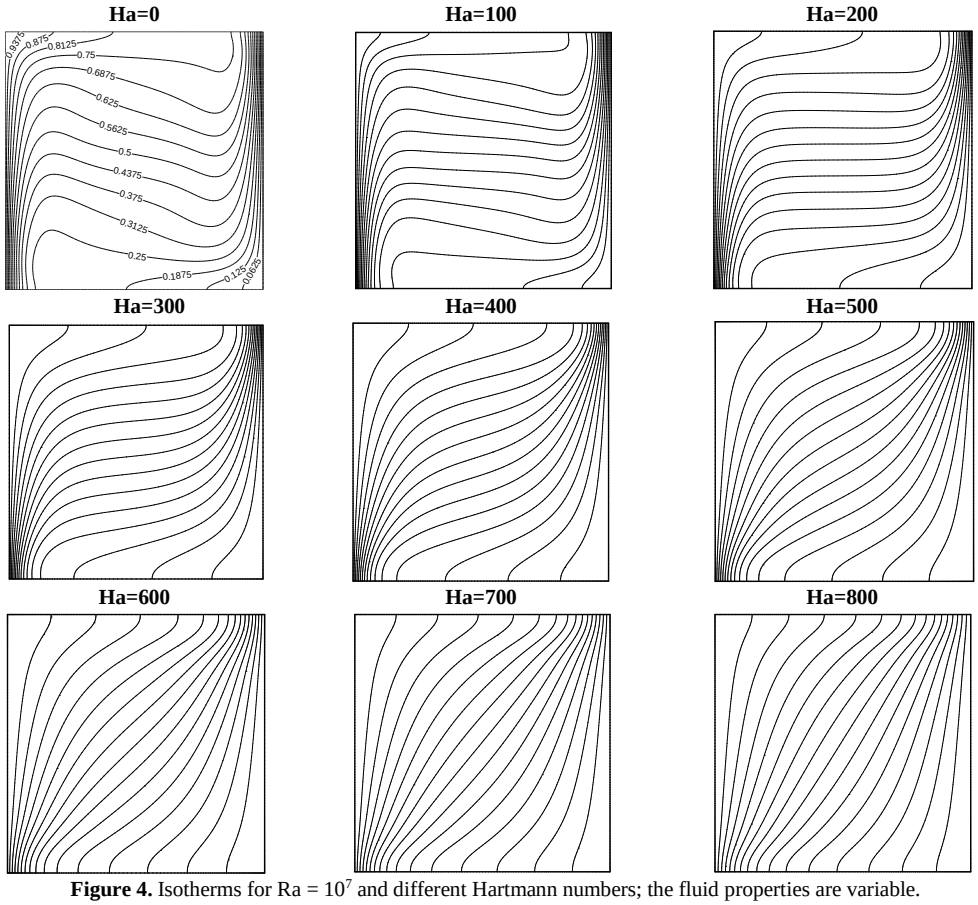

Figure 4. Isotherms for Ra = 10^7 and different Hartmann numbers; the fluid properties are variable.

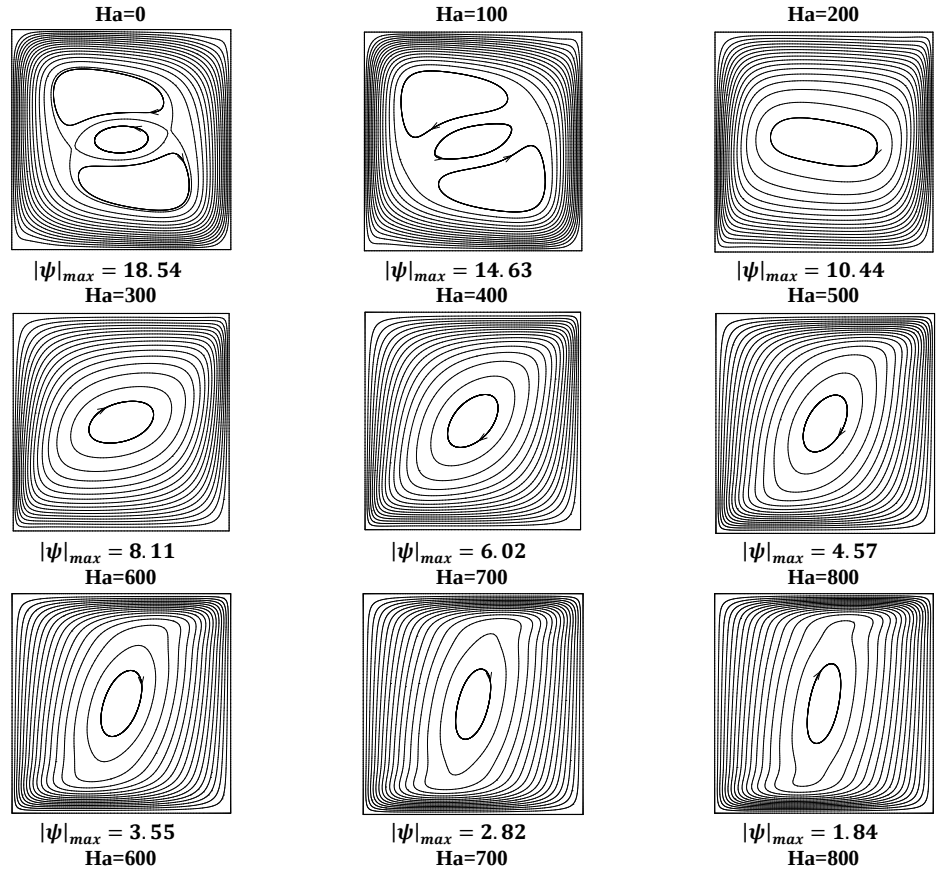

Figure 5. Streamlines for Ra = 10^7 and different Hartmann numbers; the fluid properties are constant

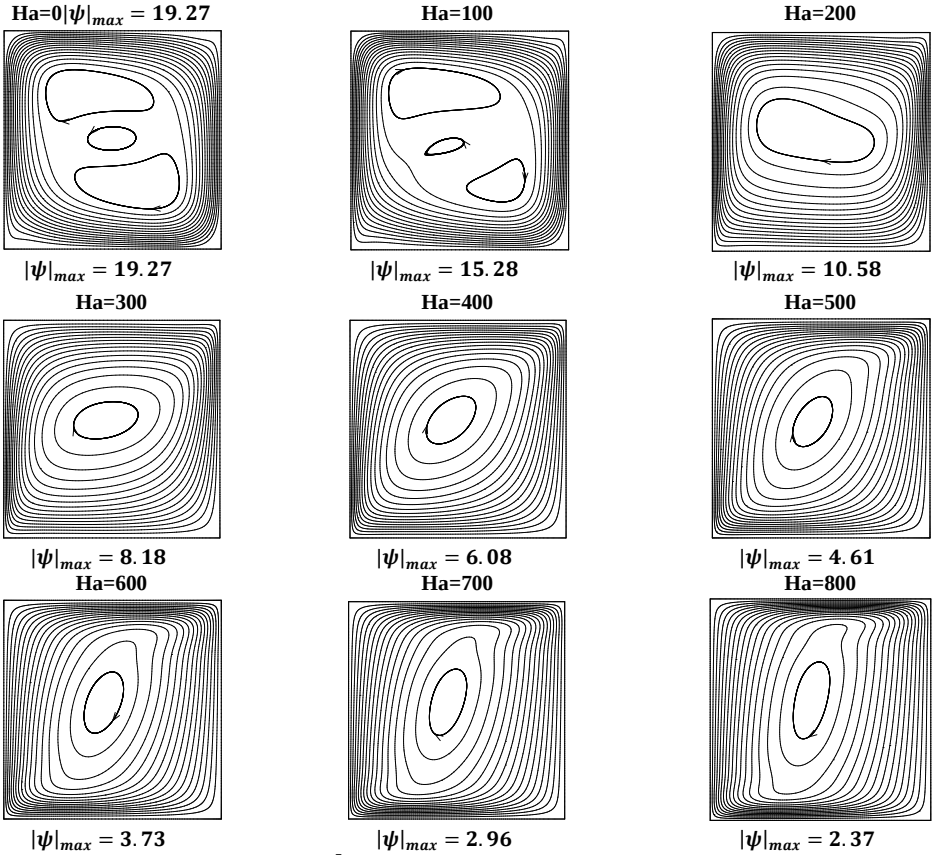

Figure 6. Streamlines for Ra = 10^7 and different Hartmann numbers; the fluid properties are variable

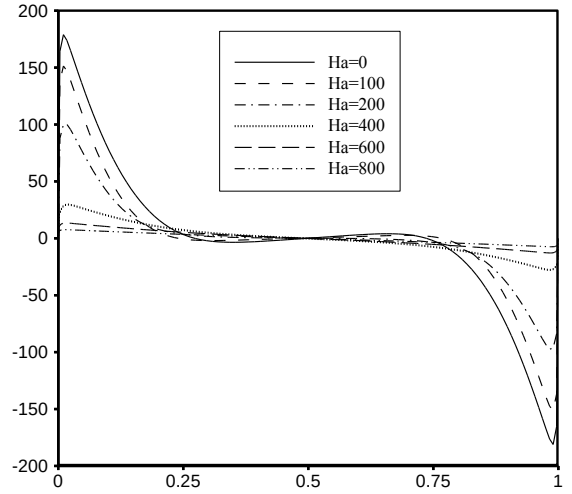

Figure 7. Velocity profile at mid height (Y=0.5) for Ra = 10^7 and different Hartmann numbers ;(a): the fluid properties are constant, (b): the fluid properties are variable.

It is perceived that for both cases the temperature gradient near the hot and cold walls and the slope of temperature profile is high as well. By applying magnetic field and increasing the Ha, the slope reduces, so at Ha=800 the profile is linear. In the case constant properties the slope of temperature profile near the vertical walls is the same and the temperature profiles pass from one point at the center of the cavity. Notwithstanding, in the case variable properties as it was expected the temperature profile don't pass one point and the slope of lines at high Hartmann numbers near the hot and cold walls are partly different. The variation of Nusselt number versus the Hartmann numbers for constant and variable properties is presented in Fig. 9.

It is observed that at both cases as Ha increases the Nusselt number decrease. However, the Nusselt number for case constant properties is more than the case variable properties. In the case constant properties, the properties at the cold wall is calculated. Regarding the equation (2) the properties have higher value rather than the case variable properties. The increasing the kinematic viscosity and electrical conductivity have reducing effect and the thermal conductivity has incremental effect on fluid flow. It is perceived from Fig.9 that the thermal conductivity has the most effect on heat transfer, so in the case constant properties convection is more than the case with the variable properties.

6. Conclusion

In the present study, turbulent MHD convection of liquid metal with constant and variable properties is investigated numerically. The following were found based on the results:

- In the case constant properties the velocity is symmetric and as Ha increases the maximum velocity decreases but in the case variable properties when Ha=0 the velocity profile is symmetric and as Ha boosts it becomes asymmetric.
- Regarding to the fact that in the case variable properties, the thermal conductivity near the hot wall is less than the cold wall and in higher Ha the diffusion mechanism is dominant and the temperature slope near the left wall is more than the right wall as well.
- In the case constant properties the slope of temperature profile near the vertical walls is the same and the temperature profiles pass from one point at the center of the cavity. Howbeit, in the case variable properties as it was expected the temperature profile don't pass one point and the slope of lines at high Hartmann numbers near the hot and cold walls are partly different.

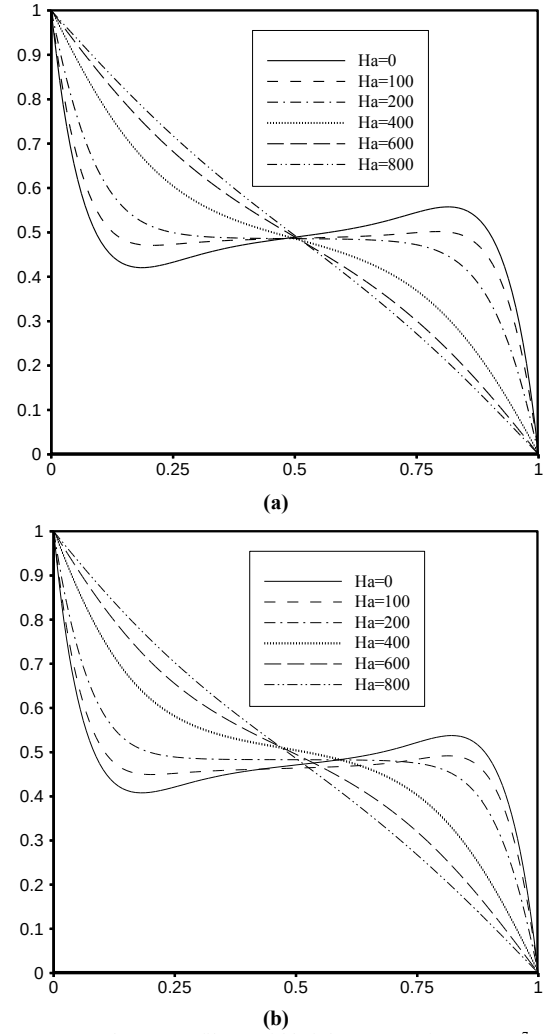

Figure 8. Isotherms profile at mid height (Y=0.5) for Ra = 10^7 and different Hartmann numbers; (a): the fluid properties are constant, (b): the fluid properties are variable.

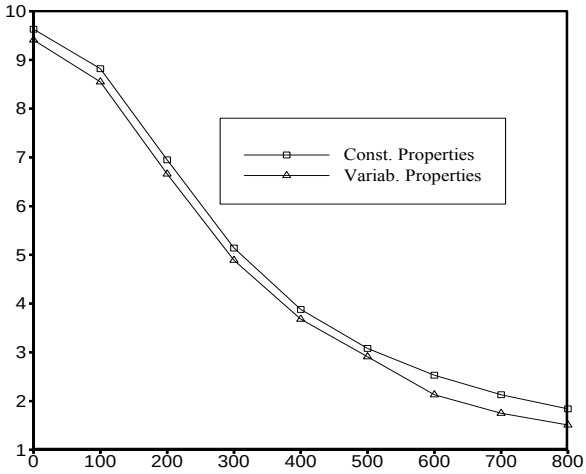

Figure 9. Variation of Mean Nusselt Number

Nomenclature

A	Magnetic potential vector (Vs/m)
B_0	Magnitude of magnetic field (kg/s² A)
Cp	Heat capacity (J/kg K)
g	Acceleration due to gravity (m/s²)
H	Height of the enclosure (m)
Ha	Hartmann number
k	Thermal conductivity (W/m.K)
P	Pressure (N/m²)
Ra	Rayleigh number
Re_m	Magnetic Reynolds number
T	Temperature (K)
u, v	The velocity components(m/s)
β	Coefficient of thermal expansion (1/K)
α	Thermal diffusivity (m²/s)
ν	Dynamic viscosity (m²/s)
ρ	Density (kg/m³)
σ	Electrical conductivity (S/m)
θ	Dimensionless temperature
μ_0	Magnetic permeability (H/m)
K	Turbulent energy (m²/s²)
ε	Dissipation rate (m²/s³)
μ_t	Turbulent viscosity (Kg/ms)

References

[1] M. D, Sozou, R.F.D,Mirando, H.A Machado, Natural convection in enclosures with variable fluid properties, International Journal of Numerical Methods for Heat & Fluid Flow, 13(8), (2003).

[2] E. Leonardi, J.A Reizes, Convective flows in closed cavities with variable fluid properties, Wiley, New York, (1981).

[3] Z.Y., Zhong, , K.T. ,Yang, J.R., Lloyd, Variable property effects in laminar natural convection in a square enclosure, ASME J. Heat Trans. 107, 133–138 (1985).

[4] M. A. Leal, H. A. Machado, R. M. Cotta, Integral transform solutions of transient natural convection in enclosures with variable fluid properties, Int. J. Heat Mass Trans. 43, 3977–3990 (2003).

[5] Y. Y. Jin, C. F. Chen, Natural convection of high Prandtl number fluids with variable viscosity in a vertical slot, Int. J. Heat Mass Trans., 39, 2663–2670(1966).

[6] S. Saravanan, P. Kandaswamy, Buoyancy convection in low Prandtl number liquids with large temperature variation, Meccanica, 37, 599–608 (2002).

[7] T. Pesso, S. Piva, ,Laminar natural convection in a square cavity: low Prandtl numbers and large density differences, Int. J. Heat Mass Transfer, 52, 1036–1043 (2009)

[8] M. Bahiraei, M. Hangi, Investigating the efficacy of magnetic nanofluid as a coolant in double-pipe heat exchanger in the presence of magnetic field Energy Conversion and Management, 76, 1125-1133 (2013).

[9] Mehdi Bahiraei, Morteza Hangi, Automatic cooling by means of thermomagnetic phenomenon of magnetic nanofluid in a toroidal loop, Applied Thermal Engineering 107, 700–708 (2016).

[10] Mehdi Bahiraei, Morteza Hangi, Flow and heat transfer characteristics of magnetic nanofluids: A review, Journal of Magnetism and Magnetic Materials 374, 125–138 (2015).

[11] Tlili, W.A. Khan, I. Khan. Multiple slips effects on MHD SA-Al2O3 and SA-Cu non-Newtonian nanofluids flow over a stretching cylinder in porous medium with radiation and chemical reaction. Results in Physics, 8, 213-22 (2018).

[12] Veera Krishna. M, G.Subba Reddy, A.J.Chamkha, "Hall effects on unsteady MHD oscillatory free convective flow of second grade fluid through porous medium between two vertical plates," Physics of Fluids, 30, p. 023106 (2018).

[13] V. Krishna.M and G.S. Reddy, Unsteady MHD convective flow of Second grade fluid through a porous medium in a

Rotating parallel plate channel with temperature dependent source, IOP Conf. Series: Materials Science and Engineering, 149, p. 012216 (2016).

[14] V. Krishna.M., M. Gangadhara Reddy, A.J.Chamkha, Heat and mass transfer on MHD free convective flow over an infinite non-conducting vertical flat porous plate, Int. Jour. of Fluid Mech. Res., 45(5), 1-25 (2018).

[15] Z. A. Khan, S. U. Haq, T. S. Khan, I. Khan, Unsteady MHD flow of a Brinkman Type fluid between two side walls perpendicular to an infinite plate, Results in Physics, 9, 1602-1608 (2018).

[16] N. S. Bondareva, et al., Magnetic Field Effect on the Unsteady Natural Convection in a Right-Angle Trapezoidal Cavity Filled with a Nanofluid, International Journal of Numerical Methods for Heat Fluid Flow, 25, 1924–1946 (2015)

[17] M. A. Sheremet, et al., Magnetic Field Effect on the Unsteady Natural Convection in a Wavy-Walled Cavity Filled with a Nanofluid: Buongiorno's Mathematical Model, Journal of the Taiwan Institute of Chemical Engineers, 61, 211–22 (2016).

[18] M. Pirmohammadi, M. Ghassemi, Effect of Magnetic Field on Convection Heat Transfer Inside a Tilted Square Enclosure, International Communications in Heat and Mass Transfer, 36, 776-780 (2009).

[19] M. Pirmohammadi, et al., 2011, Numerical Study of Hydromagnetic Convection of an Electrically Conductive Fluid with Variable Properties inside an Enclosure, IEEE Transactions on Plasma Science, 39, 516 - 520.

[20] J. M. Jalil, K. A. Al-Tae'y ,The Effect of Nonuniform Magnetic Field on Natural Convection in an Enclosure, Numerical Heat Transfer, Part A , 51, 899–917 (2007)

[21] S. C. Kakarantzas, et al., ,Natural Convection of Liquid Metal in a Vertical Annulus with Lateral and Volumetric Heating in the Presence of a Horizontal Magnetic Field, International Journal of Heat and Mass Transfer, 45, 3347-3356 (2011).

[22] X. Liu, et al., Effects of Static Magnetic Fields on Thermal Fluctuations in the Melt of Industrial CZ-Si Crystal Growth", Journal of Crystal Growth, 360, 38-42 (2012).

[23] S.Kakarantzas et al., Magnetohydrodynamic Natural Convection of Liquid Metal Between Coaxial Isothermal Cylinders due to Internal Heating, Numerical Heat Transfer, Part A, 65, 401–418 (2014).

[24] X. Zhang, O. Zikanov, Two-Dimensional Turbulent Convection in a Toroidal Duct of a Liquid Metal Blanket, Journal of. Fluid Mechanics, 779, 36-5 2(2015).

[25] H. Sajjadi, GH. R. Kefayati, ,MHD Turbulent and Laminar Natural Convection in a Square Cavity utilizing Lattice Boltzmann Method, Heat Transfer—Asian Research, 45 ,8, 795-814 (2016).

[26] Enayati, et al., Numerical Simulations of Transitional and Turbulent Natural Convection in Laterally Heated Cylindrical Enclosures for Crystal Growth, Numerical Heat Transfer, Part A, 70(11), 1195–1212 (2016).

[27] H. Versteeg, W. Malalaskera, An Introduction to Computational Fluid Dynamics", Longman scientific & technical (1995).

[28] U. Müller, L. Bühler, Magnetofluid dynamics in channels and containers, Springer, Wien, New York (2001).

[29] Jayatilleke, C. L. V, The Influence of Prandtl Number and Surface Roughness on the Resistance of Laminar Sublayer to Momentum and Heat Transfer", heat and mass transfer, 1,193(1969).

[30] S. V. Patankar, Numerical Heat Transfer and Fluid Flow, Hemisphere, Washington, DC (1980).